ELSEVIER

Journal of Alloys and Compounds 356–357 (2003) 486–489

Journal of ALLOYS AND COMPOUNDS

www.elsevier.com/locate/jallcom

First principles study of sodium–aluminum–hydrogen phases

S.M. Opalka*, D.L. Anton

United Technologics Research Center, Environmental Sciences Group, 411 Silver Lane MS 129-30, East Hartford, CT 06108, USA

Received 1 June 2002; received in revised form 12 November 2002; accepted 6 February 2003

Abstract

Heats of formation (ΔH_f) and disproportionation reaction enthalpies (ΔH_R) were computed for sodium–aluminum–hydrogen (SAH) compounds using a plane density functional methodology and pseudopotentials constructed with the projector augmented wave method. For the 0 K optimized structures, the computed ΔH_R compare favorably with available experimental data. The calculations identified ground state hydrogen positions in all known SAH phases, and two structural candidates for the lesser-known high temperature β-Na_3AlH_6 phase(s). The structures were analyzed to identify the interatomic orbital hybridizations and charge density distributions.

Keywords: Heats of formation; Disproportionation reaction enthalpies; Interatomic orbital hybridizations; Charge density distributions

1. Introduction

After their initial discovery and development [1–3], high purity sodium aluminum hydride (SAH), $NaAlH_4$, became a low cost replacement for $LiAlH_4$ reducing agents [4]. Early reports that high temperatures and hydrogen pressures, in excess of 175 °C and of 175 bar, respectively, were required for the rehydrogenation of $NaAlH_4$ [5], prevented the consideration of SAH as a viable hydrogen storage material. More recently, Bogdanović and Schwickardi [6] discovered that additions of 1–5 mol% transition or rare earth metals into SAH could be used to 'catalyze' both the hydride and dehydride reactions at temperatures below 160 °C and 152 bar. Since that time, doped SAH has become the prime material candidate for reversibly charging and discharging hydrogen at the moderate temperatures and pressures required for the fueling of transportation polymer electrolyte membrane fuel cells.

Tremendous kinetic advances have been made in accelerating solid-state SAH dehydrogenation and hydrogenation kinetics through the modification of dopant compositions and processing conditions [7–11]. However, hydride kinetics must still be increased several orders of magnitude to successfully meet the criteria set forth by the United States Department of Energy for hydrogen storage media, which cite a 5-min recharging time requirement for a material mass capable of storing 5 kg of hydrogen. Further advances are hampered by a lack of mechanistic understanding of the chemical reactions and associated phase transitions that take place during SAH hydrogenation and dehydrogenation. The structural features of the SAH phases must be resolved prior to determining the exact lattice positions occupied by the dopants. This information is needed to mechanistically probe how the dopants effectively accelerate these hydrogen-associated processes. Once established, such an understanding can be used to guide the development of SAH-derived materials to improve performance characteristics.

Numerous studies have identified many of the structural features of the different phases that are formed upon cycling SAH through varying temperature and pressure regimes. The symmetries and atomic positions of tetragonal $NaAlH_4$, monoclinic α-Na_3AlH_6 and cubic NaH have been identified through X-ray diffraction studies of hydrides and neutron diffraction studies of their deuterated analogs [12–18]. However, the assignment of exact hydrogen positions may still have some degree of uncertainty. Hydrogen positions cannot be accurately assigned from X-ray diffraction data, and they may not exactly correspond to the deuterium positions in the deuteride phases assigned with neutron diffraction [18]. In addition, there is

*Corresponding author.
E-mail address: opalkasm@utrc.utc.com (S.M. Opalka).

0925-8388/03/$ – see front matter
doi:10.1016/S0925-8388(03)00364-5

very limited information on the high temperature β-Na_3AlH_6 phase(s) observed in several studies [14,16]. In this paper, we present quantum mechanical simulations of the SAH ionic and electronic structures with the intent of supplementing existing experimentally determined structural information and to establish a foundation for SAH mechanistic studies.

2. Computational methodology

The periodic SAH structure, energy and property simulations were based upon density functional theory (DFT) with a plane wave basis set. These simulations were implemented with the VASP code, which calculates the Kohn–Sham ground state via an iterative band-by-band matrix diagonalization scheme and charge density mixing [19–21]. All calculations employed the generalized gradient approximation (GGA) of Perdew and Wang [22]. The valence electrons were explicitly represented with projector-augmented wave pseudopotentials (PAW) [23]. The pseudopotential configurations that yielded the minimum energies for all proposed SAH structures included: the {2s2 2p6 3s1] electrons in the sodium pseudopotential, the {3s2 3p1} electrons in the aluminum pseudopotential and the {1s1} electron in the hydrogen pseudopotential. Initial tests were conducted to identify the plane-wave cut off energy (780 eV) and Monkhorst–Pack special K-point set [24] for the proposed sodium alanate structures, which yielded a convergence error to well below 0.1 meV per atom.

The ground state energies and charge densities were calculated by application of sub-space diagonalization and band-by-band conjugation gradient algorithms. The 0 K ground state geometries were determined by minimizing the Hellman–Feynman forces with conjugate gradient algorithm, until all of the ionic forces were less than 0.05 eV/Å. Two different bulk relaxation methodologies were employed to locate ground state geometries for each SAH phase. In both methodologies, only relaxations that maintained the symmetry of each system were allowed. However, the lattice parameter ratios were intentionally not fixed to allow the minimum energy structure to be identified for a given volume. In the first methodology, bulk relaxations with two internal parameters: cell shape and atomic positions were made for each of a series of fixed volumes. The theoretical equilibrium volume was identified from equation of state fits to the change in energy/ion with the volume/ion. The final structure was determined by minimizing the lattice parameters and the positions using the theoretical equilibrium volume. In the second methodology, the three internal parameters (cell volume, cell shape and atomic positions) were relaxed simultaneously in a series of calculations made with progressively increasing precision.

Table 1
Calculated and experimentally determined Na–Al–H lattice parameters

Na–Al–H phase	Lattice parameter (Å)			Symmetry	β angle	Density (g/cc)
	a	*b*	*c*			
$NaAlH_4$						
Calc.	5.008	5.008	11.123	$I4_1/a$		1.29
Exp.(12)	5.021	5.021	11.346	Tetragonal		1.26
Exp.(13)	5.024	5.024	11.335	Tetragonal		1.25
Exp.(14)	5.027	5.027	11.371	Tetragonal		–
α-Na_3AlH_6						
Calc.	5.357	5.548	7.712	$P2_1/n$	89.93	1.48
Exp.(15)	5.408	5.538	7.757	$P2_1/n$	89.83	1.42
Exp.(14)	5.454	5.547	7.811	Monoclinic	89.83	–
Exp.(16)	5.46	5.61	7.80	$P2_1/n$	90.18	1.46
β-Na_3AlH_6						
Calc.	5.484	5.488	7.752	Immm		1.45
Calc.	7.755	7.755	7.755	Fm-3m		1.45
Exp.(16)	7.755	7.755	7.755	Cubic		1.45
NaH						
Calc.	4.83	4.83	4.83	Fm-3m		1.41
Exp.(17)	4.89	4.89	4.89	Fm-3m		1.37

3. Results and discussion

3.1. $NaAlH_4$

When the minimum energy predicted $NaAlH_4$ structure is viewed as a conventional tetragonal cell, as specified in Table 1 and shown in Fig. 1, the lattice consists of Al and Na ions arranged in a repeating superlattice of staggered arrays oriented in the [100] direction. The hydrogen

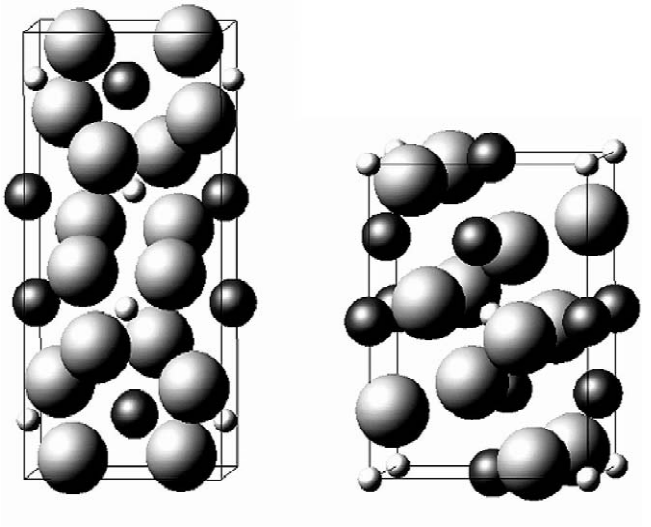

a) tetragonal $NaAlH_4$ **b)** monoclinic α-Na_3AlH_6

Fig. 1. Predicted minimum energy structures. The large gray balls are hydrogen atoms, the small light balls are aluminum atoms and the medium dark balls are sodium atoms. The images were generated with Materials Design MedeA software.

tetrahedra are distorted so that there are two different sets of opposing H–Al–H bond angles. The tetrahedra are aligned so that the hydrogens form a staggered superlattice in the [001] direction. The $NaAlH_4$ Al–H bonds are shorter than in any other SAH phase. Density of states analyses of $NaAlH_4$ revealed a single valence band predominated by the strong interaction of the Al_3p orbitals with all occupied Na and H orbitals. The valence band also contains the local hybridizations of the H_1s orbitals with: the Al_3d just below the Fermi level, Na_2p at intermediate valence energies, and Na_2s at the lowest valence energies. The electron density distribution revealed that this structure has a strong ionic character, with a minor electron density enhancement between adjacent hydrogens on neighboring AlH_4^- tetrahedra.

3.2. α-Na_3AlH_6

The monoclinic structure shown in Fig. 1 contains a pseudo-body centered cubic Al sub-lattice. Each Al atom is surrounded by a distorted octahedra of hydrogen atoms with the long octahedral axis tilted from the [001] direction towards a ⟨111⟩ direction. The octahedra apexes are oriented towards the corners of the cell and the four nearly equatorial hydrogens are aligned to form a hydrogen superlattice in the [001] direction. Density of state analyses revealed well-dispersed H_1s bonding interactions with Na and Al orbitals at intermediate energy levels. Enhanced H_1s hybridizations with the Al_3p, Al_3d, and Na_2d orbitals were observed just below the Fermi level. The electron density distribution portrayed moderate Al–H and weak Na–H covalent bonding interactions within this structure.

3.3. β-Na_3AlH_6

Two minimum energy structures were identified with the two bulk relaxation methodologies, an orthorhombic Immm structure and a cubic Fm-3m structure. The orthorhombic structure was the most energetically favorable candidate for this phase. The atomic positions in this structure are very similar to those in the monoclinic α-Na_3AlH_6 structure, except that the higher orthorhombic symmetry has enforced the alignment of the hydrogen octahedra with low index directions. The hydrogen octahedra are close to perfect symmetry, so that the octahedra orbitals are lower in energy and less dispersed. Density of states analyses showed two separate valence bands: an upper band containing the hybridized Al_3d and Na_2p energy levels of the Immm Al–Na sublattice and a split lower energy band containing the Al_3p, Na_2s and Na_2d orbitals octahedrally hybridized with H_1s orbitals. The overall electron distribution is similar to the α-Na_3AlH_6 phase, but is locally more ionic in character.

3.4. NaH

In this classic Fm-3m structure, the hydrogens were octahedrally arranged around each sodium atom. The interatomic distance between the hydrogen atoms is larger in this structure than for any other Na–Al–H phases. The H_1s orbitals are strongly hybridized with the Na_2d orbitals, just below the Fermi level. The valence electrons are ionically concentrated around the sodium atoms.

3.5. Enthalpies of formation and reaction enthalpies

The heats of formation, ΔH_f, were determined with the VASP-calculated enthalpies (H) of the constituent elements in their standard state, following the definition:

$$\Delta H_f = H_{\text{compound}} - \Sigma(\text{element compound stoichiometry} \times H_{\text{element in standard state}}) \quad (1)$$

All of the Na–Al–H hydride phases were predicted to have favorable ΔH_f values at 0 K, which are listed in Table 2. The predicted ΔH_f values at 0 K for $NaAlH_4$ and NaH are approximately two-thirds of the −112.968 and −56.379 kJ/mol values thermodynamically calculated at 298 K, respectively [27–29].

At moderate temperatures and pressures, catalyzed Na–Al–H phases reversibly and endothermically undergo

Table 2
Enthalpies of formation, ΔH_f, and reaction enthalpies, ΔH_R, predicted for the Na–Al–H phases at 0 K

Na–Al–H phase	ΔH_f kJ/mol	Reaction equation	ΔH_R kJ/mol
$NaAlH_4$	−78.85	$NaAlH_4 \rightarrow 1/3(\alpha\text{-}Na_3AlH_6 + 2Al + 3H_2)$	+20.91
α-Na_3AlH_6	−172.84	$1/3(\alpha\text{-}Na_3AlH_6) \rightarrow 1/3(\beta\text{-}Na_3AlH_6)$ Orthorhombic	+33.04
β-Na_3AlH_6 Orthorhombic	−139.80	$1/3(\beta\text{-}Na_3AlH_6) \rightarrow NaH + 1/3Al + 1/2H_2$ Orthorhombic	+19.46
β-Na_3AlH_6 Cubic	−139.79	$1/3(\beta\text{-}Na_3AlH_6) \rightarrow 1/3(\beta\text{-}Na_3AlH_6)$ Cubic Orthorhombic	+ 0.01
NaH	−38.16	$NaH \rightarrow Na + 1/2H_2$	+38.17

solid-state disproportionation reactions, releasing hydrogen and forming new hydride phases. The reactions and their corresponding enthalpies, ΔH_R, listed in Table 2 were predicted at 0 K. The ΔH_R predicted for the dehydrogenation of $NaAlH_4$ to form α-Na_3AlH_6, compares well with the value, 36.0 kJ/mol, determined from combined measurements made on pure $NaAlH_4$ at 480 K [25]. The predicted ΔH_R at 0 K for the dehydrogenation of β-Na_3AlH_6 to NaH compares well with the experimentally determined value of 13.8 kJ/mol determined at 495 K [26].

4. Conclusion

Density functional theory was used to predict energetically favorable hydrogen positions in all known SAH phases and structural candidates for the lesser-known high temperature β-Na_3AlH_6 phase(s). This information will be used to interpret how the different atomic bonding interactions contribute to the behavior of SAH compounds and to prepare for future studies of SAH catalysis mechanisms.

References

[1] H.I. Schlesinger, A.E. Finholt, US Patent 2,567,311 (1951).
[2] A.E. Finholt, British Patent 760,774 (1956).
[3] A.E. Finholt, US Patent 2,940,935 (1960).
[4] E.C. Ashby, Adv. Inorg. Chem. Radiochem. 8 (1966) 283.
[5] T.N. Dymova, N.G. Eliseeva, S.I. Bakum, Y.M. Dergachev, Dok. Akad. Nauk USSR 215 (1974) 1369.
[6] B. Bodanović, M. Schwickardi, German Patent DE 195 26 434 A1 (1997).
[7] B. Bodanović, M. Schwickardi, J. Alloys Comp. 1 (1997) 253.
[8] A. Zaluska, L. Zaluski, J.O. Ström-Olsen, J. Alloys Comp. 298 (2000) 125–134.
[9] C.M. Jensen, R. Zidan, N. Mariels, A. Hee, C. Hagen, Int. J. Hyd. Energy 24 (1999) 461.
[10] G. Sandrock, K. Gross, G. Thomas, J. Alloys Comp. 339 (2002) 299.
[11] D.L. Anton, J. Alloys Comp. (2003) in press.
[12] B.M. Bulychev, V.K. Bel'skii, A.V. Golubeva, B.M. Bulychev, V.K. Bel'skii, A.V. Golubeva, Zh. Neorg. Khim. 28 (1983) 2694.
[13] J.P. Bastide, J. El Hajri, P. Claudy, A. El Hajbi, Synth. React. Inorg. Met.-Org. Chem. 25 (1995) 1037.
[14] K.J. Gross, S. Guthrie, S. Takara, G. Thomas, J. Alloys Comp. 297 (2000) 270.
[15] E. Ronnebro, D. Noreus, K. Kadir, A. Reiser, B. Bogdanović, J. Alloys Comp. 299 (2000) 101.
[16] J.P. Bastide, B. Bonnetot, J.-M. Letoffe, P. Claudy, Mater. Res. Bull. 16 (1981) 91.
[17] G.A. Morton, W.L. Davidson, C.G. Shull, E.O. Wollan, Phys. Rev. 73 (1948) 842.
[18] Y. Fukai, in: The Hydrogen System, Springer, New York, 1993, p. 22.
[19] G. Kresse, J. Hafner, Phys. Rev. B 47 (1993) RC558.
[20] G. Kresse, J. Furthmuller, Comput. Mater. Sci. 6 (1996) 15.
[21] G. Kresse, J. Furthmuller, Phys. Rev. B 54 (1996) 11169.
[22] J. Perdew, Y. Wang, Phys. Rev. B. 46 (1992) 6671.
[23] G. Kresse, D. Joubert, Phys. Rev. B. 59 (1999) 1758.
[24] H.J. Monkhorst, J.D. Pack, Phys. Rev. B 13 (1976) 5188.
[25] C.M. Jensen, K.J. Gross, Appl. Phys. A 72 (2001) 213.
[26] P. Claudy, B. Bonnetot, G. Chahine, J.M. Letoffe, Thermochim. Acta 38 (1980) 75.
[27] M.K.h. Karapet'yants, M.L. Karapet'yans (Eds.), Calculated Using Outokumpu HSC Chemistry for Windows, Version 4.0, Using The Thermodynamic References for $NaAlH_4$, Ann Arbor–Humprey Science Publishers, London, 1970, p. 461.
[28] B. Bonnetot, G. Chahine, P. Claudy, M. Diot, J.M. Letoffe, J. Chem. Therm. 12 (3) (1980) 249.
[29] L.V. Gurvich, G.A. Bergman, L.N. Gorokhov, V.S. Iorish, V.Ya. Leonidov, V.S. Yungman, The thermodynamic data reference for NaH, J. Phys. Chem. Ref. Data 26 (4) (1997) 1031.